Eurasian ChemTech Journal 10 (2008) 1-7

Synthesis, Characterization and Catalytic Properties of Microporous Cobalt Aluminosilicate (CoLTL) Molecular Sieves

P. Selvam* and S. Rajasekar

National Centre for Catalysis Research, Department of Chemistry, Indian Institute of Technology-Madras, Chennai 600 036, India

Abstract

Thermally stable divalent cobalt substituted microporous aluminosilicate (CoLTL) molecular sieves were synthesized and characterized. These studies revealed isomorphous substitution of divalent cobalt in tetrahedral framework of LTL structure. In addition, the typical blue color of CoLTL confirms the tetrahedral environment of divalent cobalt in the framework, and as a result the catalyst showed excellent activity for the oxidation of cyclohexane under mild reaction conditions. Furthermore, unlike the many other cobalt-based microporous (heterogeneous) catalysts reported so far, CoLTL does not show any dislodgement or segregation of cobalt upon calcination or any other post-synthesis treatments. In this study, the performance of CoLTL was also compared with cobalt-containing aluminophosphate and silicate molecular sieves having AFI and MFI structures, respectively.

Introduction

Cobalt-based homogeneous catalysts such as cobalt acetate, cobalt porphyrins, cobalt phthalocyanines, cobalt bis(pyridylimino)isoindoline, etc. have been widely employed for the oxidation of cycloalkanes [1]. Attempts have also been made to substitute divalent cobalt in various silicate, aluminosilicate and aluminophosphate molecular sieves [2-6]. Among the several structure types, the most widely studied material was CoAPO-5. While the isomorphous substitution of cobalt into several APO structures is commonly accepted, there exists controversy regarding the oxidations states of cobalt in the matrix [7,8]. Numerous reports claim the incorporation of cobalt in the tetrahedral framework of molecular sieve materials but there seems to be no consistency in interpreting the exact nature of cobalt in the matrix. On the other hand, Montes *et al.* [9] have reported divalent cobalt-stabilized LTL zeolite, however, with only a small amount of cobalt in the matrix. Unlike most molecular sieve-based materials, LTL can be synthesized without the use of template molecules and hence they can be used directly. Therefore, the main objectives of this work are to synthesis and characterize CoLTL zeolite. Furthermore, the performance of this material will be evaluated for the cyclohexane oxidation under mild conditions. For a comparison, other cobalt-containing microporous catalysts such as cobalt aluminophosphate (CoAPO-5) and cobalt silicalite (Co/S-1) are also used.

Experimental

Starting Materials

Potassium hydroxide (84%, S.D Fine Chemicals), Aluminium fine powder (S.D. Fine Chemicals), Colloidal silica (Ludox, 40% suspension in water, Aldrich) and Cobalt (II) acetate (S.D. Fine Chemicals) were used as sources for alkali, aluminium, silicon and cobalt respectively. Cyclohexane (99.5%; SISCO), 2-butanone (99.5%; S.D. Fine Chemicals), H_2O_2 (30 wt.%; S.D. Fine Chemicals) and acetic acid (99.5%; Fischer) were used for reaction studies. They were used as supplied.

*corresponding authors. E-mail: selvam@iitm.ac.in

Printed in Kazakhstan

Synthesis

Cobalt-free LTL was synthesized [10] hydrothermally from a molar gel composition of $1.5K_2O:Al_2O_3:6SiO_2:37H_2O$ as per the following procedure. At first, potassium hydroxide (10 g) was dissolved in 12.5 ml distilled water and aluminium powder (2.7061 g) carefully added in small aliquots. The solution was then allowed to cool for 30 min. After homogenizing for 10 min, colloidal silica (34.75 ml) was added drop by drop. The mixture was then stirred for 60 min. The resulting gel was transferred into Teflon lined stainless steel autoclaves and kept in an air oven for crystallization. The solid product obtained was washed, filtered and dried at 323 K for 12 hrs.

Cobalt substituted LTL (CoLTL) was synthesized [9] hydrothermally from a molar gel composition of $1.5K_2O:Al_2O_3:6SiO_2:37H_2O:x$CoO where $x = 0.002$, 0.004, 0.008 and 0.0162. A typical reaction gel for an $x = 0.002$ was prepared as follows: potassium hydroxide (10 g) was dissolved in 12.5 ml distilled water and aluminium powder (2.7061 g) carefully added in small aliquots. The solution was then allowed to cool for 30 min. After homogenizing for 10 min, cobalt source was added. The mixture was then stirred vigorously for 30 min. Then, colloidal silica (34.75 ml) was added drop by drop. The resulting mixture was stirred for another 60 min. The final gel was transferred into teflon lined stainless steel autoclaves and kept in an air oven for crystallization. The solid product obtained was washed, filtered and dried at 323 K for 12 hrs. The sample is designated as CoLTL-200. The same procedure was followed for other reaction gels where $x = 0.004$, 0.008 and 0.016. The catalysts were coded as CoLTL-100, CoLTL-50 and CoLTL-25, respectively.

Cobalt-loaded LTL (Co/LTL) samples were prepared by incipient wetness method as per the following procedure. Prier to loading, LTL zeolite was activated at 383 K in an air oven for 6 hrs. An aqueous solution of cobalt (II) acetate was added dropwise to 2 g of the preactivated sample under mild stirring for 2-3 hrs. It was then washed with distilled water and dried at room temperature followed by drying at 373 K for 12 hrs. This sample is coded as Co/LTL.

Characterization

The as-synthesized and calcined samples were characterized using several analytical and spectroscopic techniques. Powder X-ray diffraction (XRD) patterns were recorded in the 2θ range of 2-50° on a Rigaku-miniflex diffractometer using a nickel filtered Cu K_α radiation ($\lambda = 1.5418$ Å). The scan speed and step size was 0.2° min^{-1} and 0.02°, respectively. The elemental compositions of the various samples were carried out by ICP-AES technique on Labtam Plasma Lab 8440 equipment. The solutions for the analysis were prepared as per the following procedure. 50 mg of dried calcined sample was taken in a platinum crucible. It is treated with 6N HNO_3, water and few drops of HF. It is then heated at 353 K in water bath for 30 min and then made to 25 ml by adding distilled water. This solution is used for ICP-AES analysis. In order to determine the stability of the as-synthesized samples, thermal analyses experiments were performed. The measurements were carried out on a simultaneous thermogravimetry/differential thermal analysis (TG-DTA; Shimazdu DT-300) in nitrogen atmosphere (40 ml/min) with 12-15 mg of the sample and a heating rate of 10 K/min in the temperature range of 300-1073 K. DRUV-VIS spectra of CoLTL samples were recorded in the range (300-700 nm) on an UV-260 Shimazdu spectrophotometer. The procedure adopted for recording the spectra is as follows: A small amount of the sample was finely ground prior to recording. It was then spread in the form of a thin and uniform layer on a Whatman 40 filter paper and then fitted on the sample holder. A blank filter paper was kept in the reference cell and used as the reference. Fourier Transform-Infrared (FTIR) spectra of the various samples were recorded on a Nicolet Impact 400 equipment with a 4 cm^{-1} resolution and 128 scans in the mid IR (400-4000 cm^{-1}) region using KBr pellet technique. About 10 mg of dry KBr was mixed with a little amount (one hundredth of the KBr amount) of the sample and ground for homogenization under IR lamp. It was then pressed into a transparent, thin pellet at 5 tons/cm^2. These pellets were used for IR spectral measurements. Scanning Electron Microscopy (SEM) imaging of the calcined samples was recorded using Cameca-Su Scanning Electron Microscope operated at 20 kV. The samples were coated with film of gold to make it conducting.

Optimization Studies

Several attempts were made to optimize the gel composition and synthesis condition. A number of samples were prepared having the following gel compositions:

i) $1.5K_2O:Al_2O_3:6SiO_2:37H_2O$;
ii) $1.3K_2O:Al_2O_3:6SiO_2:37H_2O$;
iii) $1.9K_2O:Al_2O_3:6SiO_2:67H_2O$;
iv) $9K_2O:Al_2O_3:20SiO_2:315H_2O$.

In order to optimize the crystallization time, the gel having the composition: $1.5K_2O:Al_2O_3:6SiO_2:37H_2O$ were kept at 423 K in three different autoclaves. They were taken after 1, 2 and 3 days. The crystallinity of the products is checked by XRD. In all the cases, LTL phase was obtained. However, the crystallinity of the product was low for the 1 day sample, as compared to 2 days sample where high quality phase is obtained. On the other hand, 3 days sample shows new peaks due to zeolite-z phase. The optimized crystallization time and temperature for the various LTL samples are shown in Table 1. For all other gel composition the crystallinity of the products is very low.

Catalytic Studies

The catalytic oxidation reactions were performed [11] in a round bottom glass flask under constant stirring by refluxing the reaction mixture in a temperature-controlled oil bath. The reactions were carried out at 80-100°C under atmospheric pressure for 12 hrs using 50 mg catalyst, 1.94 ml of cyclohexane, 0.47 ml of 2-butanone, 1.84 ml of aqueous H_2O_2 and 10 ml acetic acid. The reaction products are analyzed by gas chromatography (GC, Nucon 5700) using Carbowax column.

Results and Discussion

All the as-synthesized (CoLTL) samples were blue in color and it is not changed upon calcination.

Table 1
Optimized crystallization parameters for LTL structure[a]

Samples	Cobalt[b], wt.%	Crystallization conditions	
		T, K	τ, hrs
LTL	0.0	423	48
CoLTL (200)	0.95	423	48
CoLTL (100)	1.98	423	96
CoLTL (50)	3.57	438	120
CoLTL (25)	5.84	448	120

[a]Numbers in parentheses indicate the nominal [Si+Al]/Co ratios.
[b]ICP-AES data.

The respective colours of the as-synthesized as well as calcined samples showed an increase in the intensity of the colour with cobalt concentration. The XRD patterns of both Co-free LTL and CoLTL samples (Fig. 1) showed sharp and distinct reflections indicate that the samples are highly crystalline. All the reflections are indexed based on hexagonal crystal system, which is in good agreement with LTL structure [12]. The amount of cobalt present in the samples is estimated using ICP-AES technique and the results are presented in Table 1. Table 2 summarizes the structural data for the various compositions. It can be seen from this table that an increase in unit cell parameters vis-à-vis volume, suggest that the framework substitution of Co^{2+} (0.72 Å) for Al^{3+} (0.53 Å). Further, the diffraction pattern does not change after heat treatment.

The SEM of Co-free LTL and CoLTL (Fig. 2) show spherical morphology with an estimated particle size of about 2 μm. Figure 3 depicts the TG-DTA traces of LTL. It can be seen from this figure that a total weight loss of 14% is observed. The weight loss is due to removal of adsorbed water and/or other gas molecules indicating hydrophilic character of the samples. This is further supported by the endo-

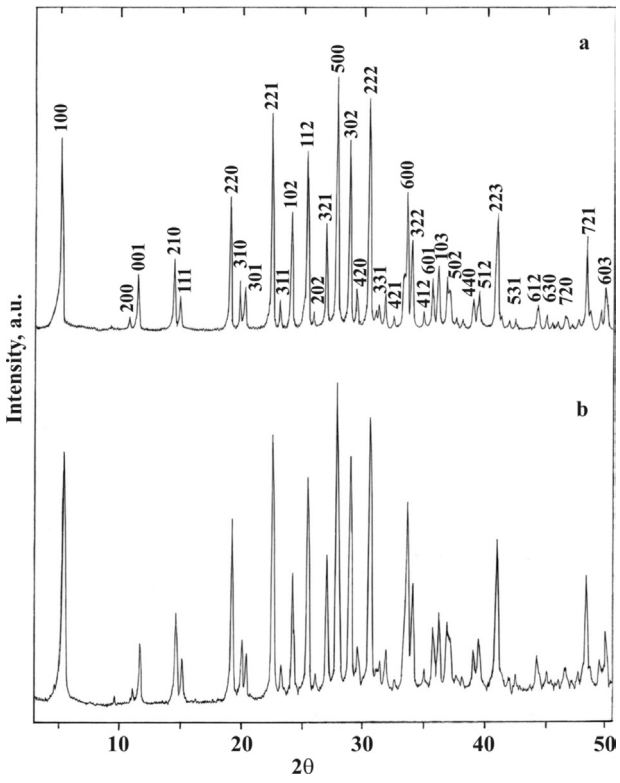

Fig. 1. XRD patterns of as-prepared: a) LTL and b) CoLTL (200).

Table 2
XRD data for LTL and CoLTL samples[a]

Catalysts	Structural data		
	a, Å	*c*, Å	*V*, Å^3
LTL	18.41	7.53	2210.2
CoLTL (200)	18.53	7.57	2251.0
CoLTL (100)	18.61	7.58	2273.5
CoLTL (50)	18.74	7.59	2308.4
CoLTL (25)	18.95	7.60	2363.5

[a]Numbers in parentheses indicate the nominal [Si + Al]/Co ratios.

thermic transition in DTA. The thermal analyses patterns of CoLTL samples (not reproduced here) are also similar to that of LTL except that the occluded water less strongly bound. This may be due to the larger size and the charge differences of Co^{2+} as compared to Al^{3+}, and as a result the polarizing capability Al^{3+} could be much greater than that of Co^2 and therefore, a lower affinity for water. This observation may be a further confirms the conjuncture that Co^{2+} substitutes Al^{3+} in the LTL structure.

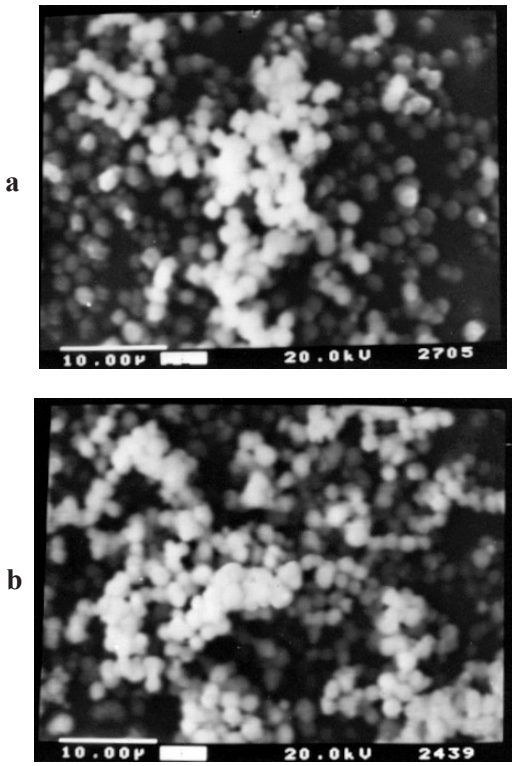

Fig. 2. SEM images of as-prepared: (a) LTL and (b) CoLTL (50).

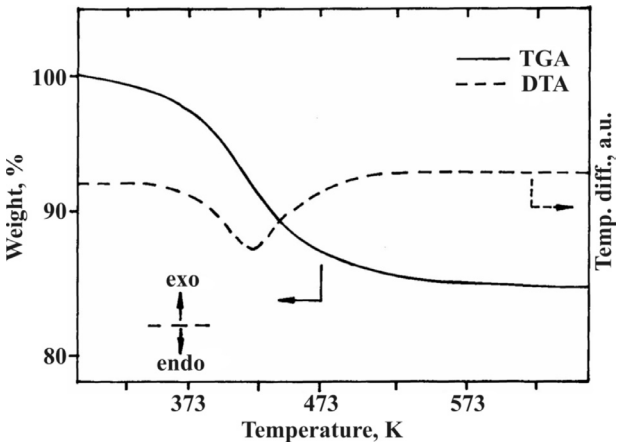

Fig. 3. Thermograms of as-prepared LTL.

The FTIR spectra of various LTL samples (not reproduced here) showed characteristic absorption bands are assigned in Table 3. It can be seen that the Si–O–T asymmetric and symmetric stretching vibrations and the T–O bending shift progressively to lower numbers on increasing cobalt content in the gel. The substitution of Al^{3+} by Co^{2+} in the zeolite framework shifts the bands toward lower wavenumbers on occunt of the larger Co–O (1.99 Å) bond distance as compared to that of Al–O bond (1.75 Å). The shift in frequency of framework vibrations to a lower wavenumber of Co^{2+} containing LTL also indicates the incorporation of Co^{2+} in the LTL lattice.

Table 3
FTIR band assignments (in cm^{-1}) of various LTL samples[a]

Samples	Asymmetric Si–O–T	Symmetric Si–O–T	Double Rings	T–O bending
LTL	1159.8	772.4	611.5	498.3
	1004.8	730.7		
CoLTL (200)	1165.7	772.4	614.5	486.4
		724.8		
CoLTL (100)	1112.1	775.4	611.5	471.5
	1022.7	733.7		
CoLTL (50)	1115.1	772.4	611.5	471.5
	1025.7	727.7		
CoLTL (25)	1109.1	724.8	608.5	471.5
	1022.7	608.6		

[a]Numbers in parentheses indicate the nominal [Si + Al]/Co ratios.

Figure 4 shows the various possible transitions of Co (II) in tetrahedral and octahedral coordination. The *d–d* transitions of Co (II) shows transitions in the infrared and visible region and the O → Co (II) charge transfer transitions in the ultraviolet region. Co (II) stays in high-spin as Co (II) coordinates with weak ligands. Δ_O and Δ_T represent the tetrahedral and octahedral ligand field splitting parameter respectively. Octahedral complexes exibit three transition from their ground state. $^4T_{1g}(F)$ $(t_{2g}^5e_g^2)$: $\nu_1 = {}^4T_{1g} \rightarrow {}^4T_{2g}(F)$; $\nu_2 = {}^4T_{1g} \rightarrow {}^4A_{2g}(F)$; $\nu_3 = {}^4T_{1g}(F) \rightarrow {}^4T_{1g}(P)$. Tetrahedral complexes also exibit three transitions from the ground state $^4A_2(F)$ $(e^4t_2^3)$: $\nu_1 = {}^4A_2(F) \rightarrow {}^4T_2(F)$; $\nu_2 = {}^4A_2(F) \rightarrow {}^4T_1(F)$; $\nu_3 = {}^4A_2(F) \rightarrow {}^4T_1(P)$. Among these transitions ν_1 always lies in the infrared region whereas the ν_2 and ν_3 transitions are often spilt into three components and are found respectively in the near infrared and visible region. All transitions in octahedral coordination are symmetry forbidden whereas for tetrahedral coordination these are symmetry and spin allowed. So, octahedral transitions are around two orders of magnitude less intense than the tetrahedral one. Here from these transitions for octahedral and tetrahedral transitions we will be discussed the coordination of the Co (II) species in the visible region (transition ν_3). Figure 5 depicts the DRUV-VIS spectra for various as-synthesized CoLTL. The samples show a triplet absorption band in visible region 540, 580, and 620 nm, which can be assigned to the $^4A_2(F) \rightarrow {}^4T_1(P)$ transition of Co (II) ion surrounded tetrahedrally by O^{2-} ions. These three can be explained by spin-orbit coupling and/or by John-Teller distortion. Similar observations are made for many other cobalt containing molecular sieves. This conforms the framework substitution of tetrahedral Co (II). For comparison the spectrum of LTL impregnated with cobalt (5 wt.%) is also shown (Fig. 5f). The absorption band is broader, less intense and does not exhibit the fine structure.

At this juncture, it is interesting to note that the DR-UV-VIS spectra of as-synthesized Co/S-1 (Fig. 6c) showed characteristic transitions corresponding to divalent cobalt in octahedral coordination, which is in accordance with the observed pink color. However, upon calcination, the color changed to pinkish blue, which may be a consequence of the formation of cobalt oxide clusters [13]. This was indicated by the increase in the absorption band at the 580 and 620 nm transitions in the calcined samples (Fig. 7c). On the other hand, upon calcinaton, no change in

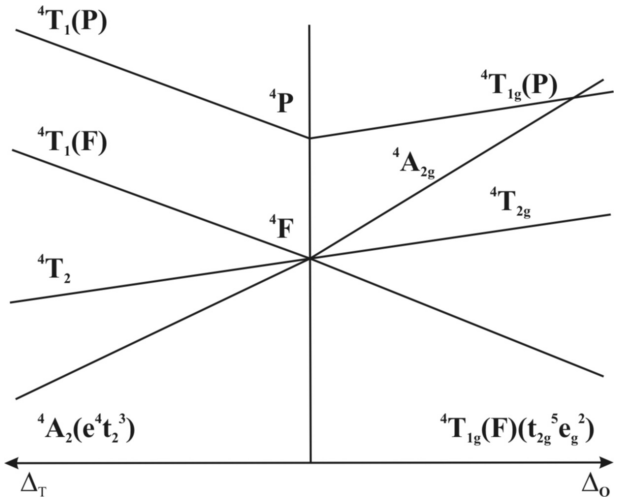

Fig. 4. Energy-level diagram of Co (II) in a tetrahedral and octahedral ligand field.

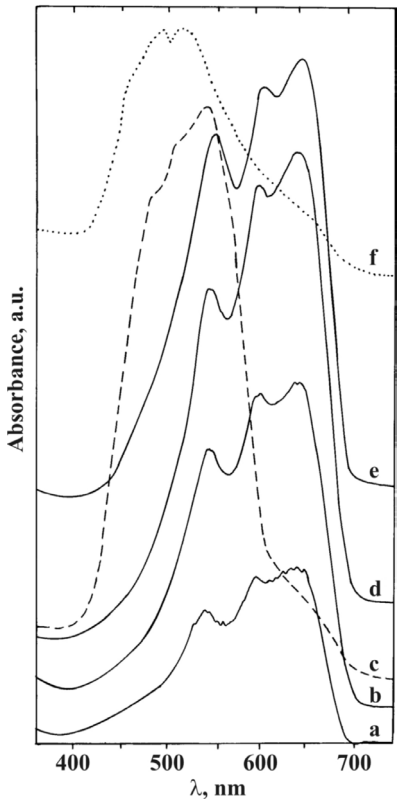

Fig. 5. DRUV-VIS spectra of as prepared: a – CoLTL (200), b – CoLTL (100), c – Cobalt acetate, d – CoLTL (50), e – CoLTL (25) and f – Co/LTL.

the spectral pattern was observed for CoLTL (Fig. 7a), whereas CoAPO-5 (Fig. 7b) shows a significant reduction in overall intensity of the visible triplet band, with the appearance of an additional new band in the UV region. The band at 370 nm is, in general,

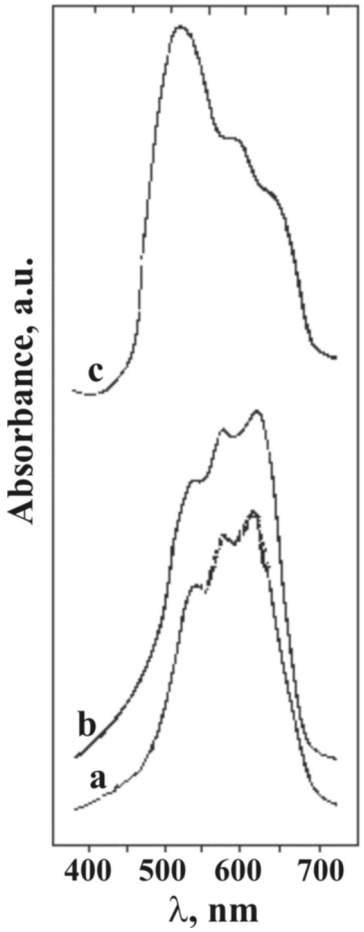

Fig. 6. DRUV-VIS spectra of as-prepared: (a) CoLTL; (b) CoAPO-5; (c) (Co)/S-1.

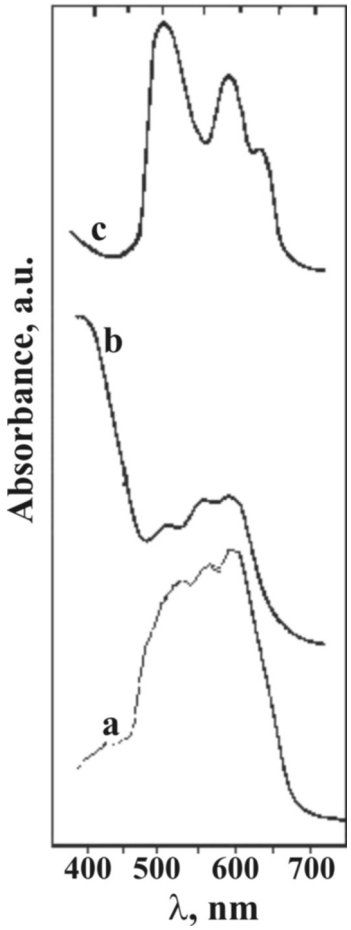

Fig. 7. DRUV-VIS spectra of: calcined: (a) CoLTL; (b) CoAPO-5; (c) (Co)/S-1.

assigned either to a transformation of symmetrical divalent tetrahedral cobalt to highly distorted tetrahedral coordination [14] or to a possible oxidation of divalent cobalt to trivalent cobalt [15].

Table 4 summarizes the results of oxidation of cyclohexane over various LTL samples. It can be seen from the table that with increasing cobalt contents the catalytic activity increases. LTL and blank results did not show any significant activity. Most importantly, in all the cases cyclohexanol selectivity is very high with low selectivity for cyclohexanone and cyclohexyl acetate. The high activity used be attributed to isolated tetrahedral Co(II) in the matrix. To check the stability of Co(II) ions in the matrix, recycling studies were carried out. No significant loss in activity was noticed. Thus, CoLTL catalysts found as highly active and truly heterogeneous catalyst. The reaction was also carried out over CoAPO-5, and Co/S-1 and the results are shown in Table 5. It can be seen from the table that the order of activity is CoLTL > CoAPO-5 > Co/S-1. It is noteworthy here that Co/S-1 showed the least activity while the activity decreased upon recycling of CoAPO-5 as a considerable amount of cobalt is leached to the reaction mixture.

Table 4
Oxidation of cyclohexane over CoLTL catalyst

Samples		Selectivity			
		Conversion	Cyclohexanol	Cyclohexanone	Others
CoLTL-50	Calcined	73.7	82.0	15.4	2.6
	Recycled[a]	72.9	84.2	13.8	2.0
CoLTL-100		55.3	88.4	8.1	3.5
CoLTL-200		43.0	92.8	5.4	1.8
LTL		7.8	85.0	2.0	13.0

[a]3-rd recycle or 4-th run.

Table 5
Oxidation of cyclohexane over various cobalt containing catalysts[a]

Catalysts		Conversion, wt.%	Co content[b], wt.%	Selectivity, wt.%		
				-ol	-one	Others
CoLTL (50)[c]	Calcined	73.7	3.57	82.0	15.4	2.6
	Recycled	72.9	3.52	84.2	13.8	2.0
CoAPO-5 (50)[d]	Calcined	78.9	3.20	81.6	17.3	6.1
	Recycled	50.8	2.62	80.2	15.1	4.7
Co/S-1 (50)[e] Calcined		41.2	1.90	85.7	6.7	7.6
No catalyst		9.0	---	78.1	---	---
CoO		28.3	78.60	79.4	10.0	10.0
$Co(CH_3COO)_2 \cdot 4H_2O$		95.0	23.65	44.0	38.0	38.0

[a]Reaction conditions: substrate:oxidant (H_2O_2) = 1:1; catalyst = 50 mg (3.3 wt.%); solvent = acetic acid (10 ml); MEK = 5 mmol; temperature = 373 K; time = 12 hrs. [b]From ICP-AES analysis; 3-rd recycle or 4-th run. [c][Si + Al]/Co = 50. [d][Al + P]/Co = 50. [e]Si/Co = 50.

Conclusions

CoLTL zeolite was successfully carried out with optimized synthesis parameters. The various physico-chemical studies confirm the isomorphous substitution of divalent cobalt in the framework structure. Interestingly, unlike, many other cobalt-containing microporous materials, no colour change was observed upon heat treatment indicating the stabilization of Co (II) ions in the matrix. Remarkable conversion (cyclohexane) and product (cyclohexanol) selectivity was obtained as compared to several heterogeneous catalysts. Further, unlike the other cobalt-based systems, the cobalt ions in remain intact, and that the active cobalt ions do not leach out even after recycling experiments. Hence, CoLTL behaves truly as heterogeneous catalyst.

Acknowledgement

The authors thank SAIF, IIT-Bombay for ICP-AES and SEM measurements. Thanks are also due to Dr. S.K. Mohapatra for the experimental assistance.

References

1. Sheldon, R.A., and Kochi, J.K., Metal Catalysed Oxidation of Organic Compounds, Academic Press, New York, 1981.
2. Lin, S.-S., and Weng, H.-S., Appl. Catal. A 105: 289 (1993); 118:21 (1994).
3. Vanoppen, D. L., De Vos, D.E., Genet, M.J., Rouxhet, P.G., and Jacobs, P.A., Angew. Chem. Int. Ed. Engl. 34:560 (1995).
4. Thomas, J.M., Raja, R., Sankar, G., and Bell, R.G., Acc. Chem. Res. 34:191 (2001).
5. Selvam P., and Mohapatra, S.K., J. Catal. 233: 276 (2005).
6. Hamdy, M.S., Ramanathan, A., Maschmeyer, T., Hanefeld U., and Jansen, J.C., Chem. Eur. J. 12:1782 (2006).
7. Hartmann M., and Kevan, L., Chem. Rev. 99: 635 (1999).
8. Weckhuysen, B.M., Rao, R.R., Martens, J.A. and Schoonheydt, R.A., Eur. J. Inorg. Chem. 565 (1999).
9. Montes, C., Montes, V.C., Villa A.L., and Corredores, N.M.R., Appl. Catal. A 197:151 (2000).
10. Wan, Y., Williams, C.D., Duke C.V.A., and Cox, J.J., Micropor. Mesopor. Mater. 47:79 (2001)
11. Sakthivel A., and Selvam, P., J. Catal. 210:134 (2002).
12. Barrer R.M., and Villiger, H., Z. Kristallogr. 128:270 (1969).
13. Jentys, A., Pham, N.H., Vinek, H., Englisch, M., Lercher, J.A., Micropor. Mater. 6:13 (1996).
14. Weckhuysen, B.M., Verberckmoes, A.A., Uytterhoeven, M.G., Mabbs, F.E., Collison, D., Boer, E., Schoonheydt, R.A., J. Phys. Chem. B 104:37 (2000).
15. Frache, A., Gianotti, E., Marchese, L., Catal. Today 77:371 (2003).

Received 12 February 2007